Sensitivity of fish stock trajectories to climate forcing and human exploitation at a global scale

Raphaël Benerradi, Vasilis Dakos, Alejandro V Cano

Sensitivity of fish stock trajectories to climate forcing and human exploitation at a global scale

Raphaël Benerradi [1,2] **Vasilis Dakos** [1] **Alejandro V Cano** [1,*]
[1] Institut des Sciences de l'Évolution de Montpellier (ISEM), Univ. de Montpellier, CNRS, IRD, Montpellier, France
[2] LIRMM, INRIA, Univ Montpellier, CNRS, Montpellier, France
[*] Correspondence: alejandro.viloria-cano@umontpellier.fr

ABSTRACT

Global fisheries are under increasing pressure from overfishing and climate change, threatening marine biodiversity and food security. Disentangling the impacts of these two drivers is essential for sustainable management, yet it remains a major challenge due to the complex nature of marine ecosystems. Here, we utilize a data-driven Empirical Dynamic Modeling EDM) framework to assess causal relationships between harvest rate, sea surface temperature SST), and the productivity of 155 fish stocks worldwide. Our analysis identifies fishing pressure as the most prevalent driver of stock productivity, with a causal link detected in 73 stocks. SST was also identified as a significant driver of productivity in 41 stocks. While the impact of harvest rate was stock-specific, being either positive or negative, the influence of SST was predominantly negative and, in many cases, intensifying over time. These results provide empirical evidence that direct exploitation and climate warming are systematically impacting fish stock productivity.

INTRODUCTION

Fisheries are a vital component of global food security, yet their sustainability is under significant threat. The proportion of marine stocks fished within biologically sustainable levels continues to decline, reaching just 62.3% of sustainably fished stocks in 2021 [1]. Among the various drivers affecting fish stock trajectories, fishing pressure is a major one. Climate change has impacts on marine fish stocks and ecosystem services – especially food provisioning – through warming temperatures affecting stock distribution and productivity, acidification, deoxygenation, shifts in primary productivity or influxes of particulate organic carbon (POC) [2–6]. Crucially, these drivers are not independent; overfishing can amplify the vulnerability of fish stocks to climate impacts, undermining their resilience and long-term viability [2,3,7].

Yet, identifying the global drivers of fish stocks and their relative importance remains a challenging and difficult task [8]. The Intergovernmental Science-Policy Platform on Biodiversity and Ecosystem Services (IPBES) Global Assessment provides an estimate of the relative importance of the drivers of global decline in marine ecosystems based on a meta-analysis that identifies direct exploitation as the most important driver, followed by changes in ocean use and climate change [9]. While the attribution methodologies provide outstanding information on the drivers of biodiversity change, they mostly rely on mechanistic models, species distribution models, controlled environment experiments and expert knowledge – e.g. thresholds identified by ecophysiology. These methods allow us to consider a wide range of information through knowledge of the effects involved. However, few studies seem to consider the inference of global causal effects based on data-driven frameworks [10,11].

Here, we employ a data-driven framework and infer causality directly from empirical time series. Specifically, we apply Empirical Dynamic Modeling (EDM) to a global database of 155 commercially exploited fish stocks to assess and quantify the causal drivers of stock productivity. We use Convergent Cross-Mapping (CCM), strengthened with a stringent null model testing procedure, to identify causal links between stock productivity and two key drivers: fishing pressure (harvest rate) and sea surface temperature. We then quantify the direction, strength, and temporal trend of these detected causal effects. This data-driven non-parametric (i.e. equation-free) approach allows us to investigate the non-linear dynamics governing fisheries and provide a robust, large-scale assessment of the sensitivity of marine ecosystems to both human exploitation and environmental forcing.

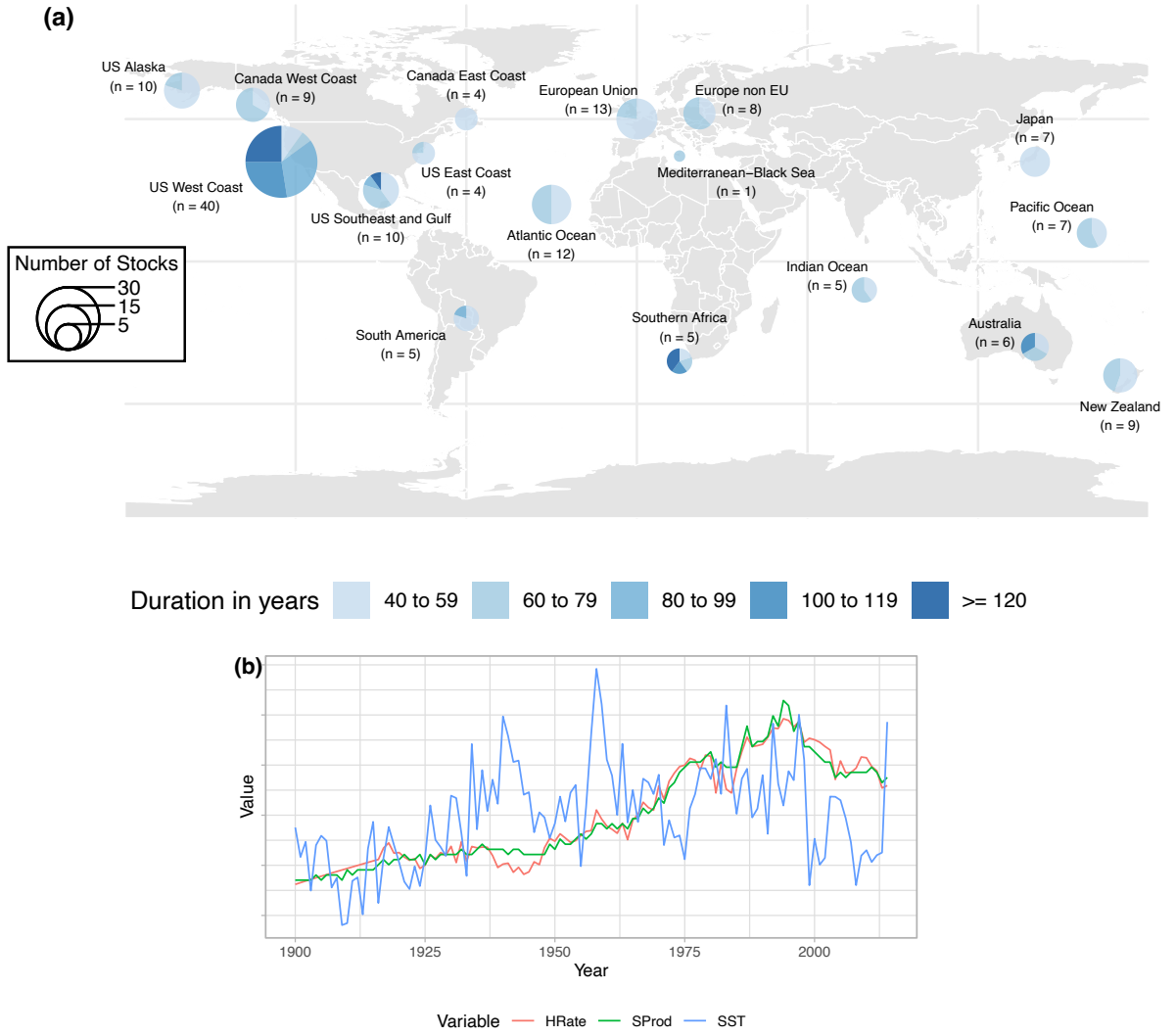

Figure 1: Overview of the processed dataset from the RAM Legacy Database. (a) Pie charts of duration of the timeseries located at the region of the fish stock, for the 155 fish stocks analyzed in this study. (b) Example of the timeseries for the fish stock *China rockfish Southern Pacific Coast*; Rate is the harvest rate (U) normalized by the harvest rate a the maximum sustainable yield (U_{MSY}), SST is centered and scaled, and stock $SProd$ is the surplus productivity divided by the mean total biomass along time.

METHODS

Dataset

We used the RAM Legacy Stock Assessment Database version v4.66 (RAMLDB) which consists of fishery-related data for 1594 commercially exploited marine fish and invertebrate stocks[12]. This dataset provides the annual time series of total biomass, total catch and harvest rate. Based on the total biomass and total catch, we computed time series of the stock productivity (SProd) for each year for each stock. Productivity quantifies the biomass produced by a fish stock that exceeds what is needed for its own reproduction and maintenance, hence representing a measure of the ability to sustainably support future harvesting. It is defined as follows: $\mathrm{SProd}\ t) =$ TB $t+1)$ TB $t)+$TC $t)$, where $\mathrm{SProd}\ t)$ is the productivity at time t, TB the total biomass, and TC the total catch[13,14]. We then divided the productivity by the average total biomass of the fish stock along the timeseries, to normalize the surplus production relatively to the average size of the fish stock.

In the RAMLDB, harvest rate refers to either exploitation rate or fishing mortality. We use the harvest rate U normalized by the harvest rate at the maximum sustainable yield (MSY) biological reference point (BRP) U_{MSY}, derived from stock assessment models. This normalized harvest rate is denoted as Rate. Specifically, $\mathrm{Rate} = U/U_{MSY}$. Thus, a fish stock with $\mathrm{Rate} = 1$ is at the management target reference point, a fish stock with $\mathrm{Rate} > 1$ is overfished with respect to the harvest rate, and underfished if $\mathrm{Rate} < 1$.

Sea Surface Temperature (SST) was extracted from the Met Office HadISST1 dataset [15]. To match the SST to each fish stock, we collected the geographic boundaries of the stocks in the RAMLDB, available at Christopher Free's website: https://chrismfree.com/ram-legacy-stock-boundary-database/. For each fish stock and for each year, we computed the geographic average within the fish stock boundary of the annual average of SST. We only kept fish stocks with more than 40 consecutive years of data for productivity, harvest rate and SST, as previously done in the application of the EDM framework on fish stocks [16,17]. After filtering, we got 155 fish stocks for analysis. An overview of the dataset is presented in Figure 1. We conducted the analysis in R version 4.4.2, mainly using the R package `rEDM` version 1.15.4.

Embedding dimensions - Simplex projection

Empirical Dynamical Modeling (EDM) relies on representing the dynamics of a system – i.e. multiple variables changing through time – by using delay embeddings – a single variable with its lags changing through time. Simplex projection allows to assess the quality of this representation. Let us consider timeseries of n variables associated to a given fish stock for each time step t from 1 to T: $x_1\ t), \ldots, x_n\ t)))_{t\in\{1,\ \ ,T\}}$. For instance, in our case, $n = 3$ and x_1, x_2, and x_3 are SST, Rate, and SProd. According to Takens' Theorem [18], for any $j \in \{1, \ldots, n\}$, there exist an integer E_{optimal} such that the manifold in the state space $x_1\ t), \ldots, x_n\ t)))_{t\in\{1,\ \ ,T\}}$ is isomorphic to the manifold in the lag space $x_j\ t), x_j\ t\ \ 1), \ldots, x_j\ t\ \ E_{\text{optimal}}+1)))_{t\in\{E_{\text{optimal}},\ \ ,T\}}$. In practice, E_{optimal} is defined based on the Simplex projection algorithm from the EDM framework (see supplementary material of Sugihara et al. 2012 [19]).

The Simplex projection aims at predicting future values of a variable based on nearest neighbors in the lag space. More precisely, $\hat{x}_j\ t+1)$ is predicted based on the next value of the nearest neighbors of $x_j\ t), x_j\ t\ \ 1), \ldots, x_j\ t\ \ E+1))$, among all other time steps $x_j\ s), x_j\ s\ \ 1), \ldots, x_j\ s\ \ E+1)))_{s\neq t\ ,\ E\leq s\leq T}$. We get a forecasting skill $\rho\ E)$, defined as the correlation between the observed $x_j\ t+1))_t$ and the predicted $\hat{x}_j\ t+1))_t$ over all time steps t. We tried embedding dimensions E from 2 to 10 to search for the optimal E_{optimal} that was associated with a high forecasting skill $\rho\ E_{\text{optimal}})$ [19]. To define E_{optimal}, we consider the trade-off of E_{optimal} being small enough and providing a sufficiently high forecasting skill, by selecting the smallest E in the top 20% of forecasting skills. That is, let us note $\rho_{min}^{\ sat)} = \max\ \ 0\ ,\ \min_E\ \rho\ E))\ )$ and $\rho_{max} = \max_E\ \rho\ E))$. We selected $E_{\text{optimal}} = \min\left\{E\ ;\ \rho\ E) \geq \rho_{min}^{\ sat)} + 0.8 \times\ \rho_{max}\ \ \rho_{min}^{\ sat)}\right\}$. The minimum forecasting skill considered is saturated at 0 because a negative forecasting skill means the embedding is not relevant to represent the dynamics in the lag space. If all the forecasting skills $\rho\ E))_{E\in\{2,\ \ 10\}}$ are negative, we consider that no embedding dimension allows to represent properly the dynamics. The Simplex projection was applied using the `EmbedDimension` function from the R package `rEDM`.

Causality assessment - Convergent Cross Mapping CCM)

Convergent Cross-Mapping (CCM) is a method to identify causality between variables in non-linear dynamical systems that don't verify separability – i.e. the information of a causal variable is not independently unique to this variable [19]. Here, considering the dynamics $\frac{d\mathbf{x}}{dt}\ t) = f\ \ x_1\ t), \ldots x_n\ t)), t)$, x_i causing x_j refers to the dependence on x_i in the j^{th} coordinate of f [11]. Note that here, the definition of causality doesn't refer to causality found from experimental design.

In the EDM framework, causality from variable x_i to variable x_j can be assessed if we can predict some information on $x_i\ t)$ from $x_j\ t), x_j\ t\ \ 1), \ldots, x_j\ t\ \ E_{\text{optimal}}+1))$. x_i is generally referred to as the target variable, and x_j the library variable. We can predict the target variable $x_j\ t)$ at a given time $t \geq E_{\text{optimal}}$ based on the $E_{\text{optimal}}+1$-nearest neighbors of $x_j\ t), x_j\ t\ \ 1), \ldots, x_j\ t\ \ E_{\text{optimal}}+1))$ in the lag space among all the possible other time steps $x_j\ s), x_j\ s\ \ 1), \ldots, x_j\ s\ \ E_{\text{optimal}}+1)))_{s\neq t\ ,\ E_{\text{optimal}}\leq s\leq T}$. This means using a library size $L = T\ \ E_{\text{optimal}}$ ($T\ \ E_{\text{optimal}}$ points considered in the lag space) to find the corresponding time steps $s\ 1), \ldots, s\ E_{\text{optimal}}+1)$ of the nearest neighbors in order to predict $\hat{x}_i\ t)$ as a weighted average of the $x_i\ s\ 1)), \ldots, x_i\ s\ E_{\text{optimal}}+1))$. Similar to the Simplex projection described above, we define a forecasting skill ρ as the correlation between the observed $x_i\ t))_t$ and the predicted $\hat{x}_i\ t))_t$ over all time steps t. We can repeat this set of predictions for various library sizes L, by randomly picking L time steps that will be the only ones considered for the nearest neighbors. We applied 100 bootstraps of this random subsample of time steps for 20 library sizes L regularly distributed from 5 to $T\ \ E_{\text{optimal}}$. Since the CCM relies on E_{optimal} for the library variable, if no embedding dimension was found relevant in the Simplex projection, no causality can be assessed from any variable to this library variable.

The causality was assessed in two successive tests detailed below. First, the assessment of causality requires an increase in the fore-

casting skill ρ with increasing library sizes L[20]. We applied a Mann-Kendall test[21] to check for a monotonic increase on the median of the forecasting skill over the 100 bootstraps along the library size, i.e. on $L \mapsto \text{median}\{\rho \text{ library set})\}_{\text{library size}=L}$. If $\tau > 0$ and p-value < 0.05, the first step of the procedure is considered successful[17].

To ensure that the forecasting skill $\rho\ L)$ resulted from the temporal structure of the time series, we compared the output of the CCM from the original time series to the output of a null model[20,22]. We generated surrogate time series by randomly shuffling time for the cause and the consequence variables: given a permutation σ of $\{1,\dots,T\}$, we considered the time series $x_i\ \sigma\ 1)),\dots,x_i\ \sigma\ T))$ and $x_j\ \sigma\ 1)),\dots,x_j\ \sigma\ T))$. We applied CCM to compute a forecasting skill for each library size across all 100 surrogate time series, using a single bootstrap per surrogate. Then, the second test to assess causality was passed if the median forecasting skill in the original time series was higher than the 95^{th} percentile forecasting skill in the surrogates, for at least 18 out of 20 library sizes.

If both the Mann-Kendall test and the comparison with surrogates were passed, we concluded that there is causality from x_i to x_j. An example of CCM that passed both tests, and another that failed both tests is presented in Figure 2. The CCM was applied using the `M` function from the R package `rEDM`.

Note that CCM should be able to distinguish causality between a variable a to another variable b, from causality of a third variable c forcing both variables a and b[19]. We assessed causality from SST to SProd and from Rate to SProd. For a consistency check, we also assessed causality from SProd to SST and from SProd to Rate – that aren't expected to occur.

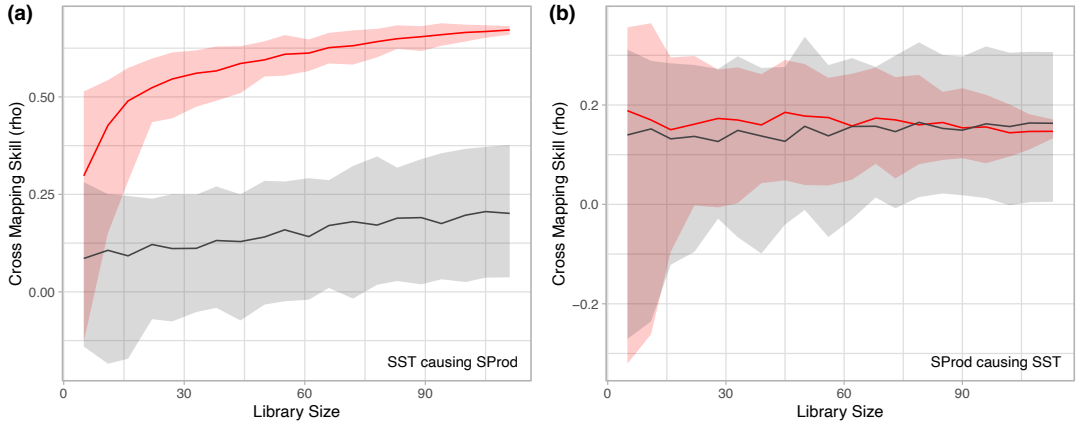

Figure 2: Convergence in the Convergence Cross Mapping CCM) for the causality between SST and stock SProd for the stock *hina rockfish Southern Pacific oast*. Both directions of causality are tested: SST (target variable) causing SProd (library variable) (a) and SProd (target variable) causing SST (library variable) (b). The red curves correspond to the CCM on the original data with 100 bootstraps (solid line for the median and ribbon for the 5^{th} and 95^{th} percentiles of the bootstraps). It represents the forecasting skill of the target variable given various number of points included in the library variable. The grey curves correspond to the 100 surrogates (solid line for the median and ribbon for the 5^{th} and 95^{th} percentiles of the surrogates). Mann-Kendall's are $\geq$ .999 and .442 with corresponding p-values of $\leq 1\ ^{6}$ and . 7, for the causality from SST to SProd (a) and from SProd to SST (b), respectively. Median forecasting skill is higher than the 95^{th} percentile of the surrogates for all of the 20 library sizes for the causality from SST to SProd (a) and for none of the library sizes for the causality from SProd to SST (b).

Quantification of the causal effect - Multivariate S-map forecasting

We applied the multivariate S-map forecasting to quantify the strength of causality for pairs of variables where we identified causality using CCM (see section above)[23,24]. The multivariate S-map aims at linearly approximating the dynamics in an embedding relevant for the causality we consider. The embedding should be of dimension E_{optimal} of the library variable (consequence variable) since it is better suited for studying the corresponding causality. This embedding space to study the strength of causality from x_i to x_j contains values associated to each time steps t, starting with the dimensions $x_i\ t)$ the cause variable at time t, $x_j\ t)$ the consequence variable at time t. Then if $E_{\text{optimal}} > 2$ we also consider the third variable at time t if the causal relationship was found significant for the third variable causing x_j. If the number of variables doesn't reach E_{optimal}, we add the lags of the consequence variable $x_j\ t \quad u)$ for $u \in \ ^{*}$ from 1 until the number of variables in the embedding reaches E_{optimal}[11,25].

Let us note $z_1,\dots,z_{E_{\text{optimal}}}$ the scaled variables in this embedding ($z_1 = \frac{x_i \quad \text{mean}_t\ x_i)}{\text{std}_t\ x_i)}$, $z_2 = \frac{x_j \quad \text{mean}_t\ x_j)}{\text{std}_t\ x_j)}$, and the other variables as explained above). The dynamics $z_2\ t) = g\ z_1\ t),\dots,z_{E_{\text{optimal}}}\ t))$ is linearly approximated by $z_2\ t+1) \approx c_0^{\ t)} + c_1^{\ t)}\ z_1\ t) + \ \dots \ +$ $c_{E_{\text{optimal}}}^{\ t)}\ z_{E_{\text{optimal}}}\ t)$. The coefficients $c_0^{\ t)},\dots,c_{E_{\text{optimal}}}^{\ t)}$ are fitted using all time steps in a weighted linear regression, with weights decreas-

ing exponentially:

$$w_k^{t)}\ \hat{z}_2^{t)}\ k+1) = w_k^{t)} c_0^{t)} + w_k^{t)} c_1^{t)}\ z_1\ k) + w_k^{t)} c_2^{t)}\ z_2\ k)\ +\ \ldots\ +\ w_k^{t)} c_{E_{\text{optimal}}}^{t)}\ z_{E_{\text{optimal}}}\ k) \tag{1}$$

$$\text{with}\quad w_k^{t)} = \exp\left\{ \frac{\|\ \ k)\quad\quad t)\|}{\frac{1}{T}\sum_{l=1}^{T}\|\ \ l)\quad\quad t)\|} \right\},\quad \text{noting}\quad\quad = z_1, \ldots, z_{E_{\text{optimal}}}) \tag{2}$$

where $k \in \{1, \ldots, T\}$ are all the time steps, $c_0^{t)}, \ldots, c_{E_{\text{optimal}}}^{t)}$ are the parameters of the regression for the time step t, $\left(w_k^{t)}\right)_{k\in\{1,\ \ ,T\}}$ are weights decreasing exponentially with a non-linear parameter – representing how local is the information in the manifold. We applied the S-map with between 0 and 20 in increments of 0.2. We then chose that provided the highest forecasting skill – defined as the correlation between the observed $z_2\ t+1))_t$ and the predicted $\hat{z}_2^{t)}\ t+1))_t$. The multivariate S-map forecasting was applied using `SMap` function from the R package `rEDM`.

The coefficient $c_1^{t)}$ is therefore the S-map coefficient informing on the strength of causality from x_i to x_j at time t. We applied a t-test on the coefficients $c_1^{t)})_{t\in\{1,\ \ ,T\ \ 1\}}$ to identify a non significant sign (p-val > 0.05), a positive sign (p-val ≤ 0.05 and positive mean), negative sign (p-val ≤ 0.05 and negative mean) of the S-map coefficients. We also applied a linear regression on $c_1^{t)})_{t\in\{1,\ \ ,T\ \ 1\}}$ depending on t, to identify a non significant trend (p-val > 0.05 of the model), a positive trend (p-val ≤ 0.05 and positive linear coefficient on t), negative trend (p-val ≤ 0.05 and negative linear coefficient on t) of the S-map coefficient. An example of the coefficients along time, t-test and linear regression are presented in Figure 3.

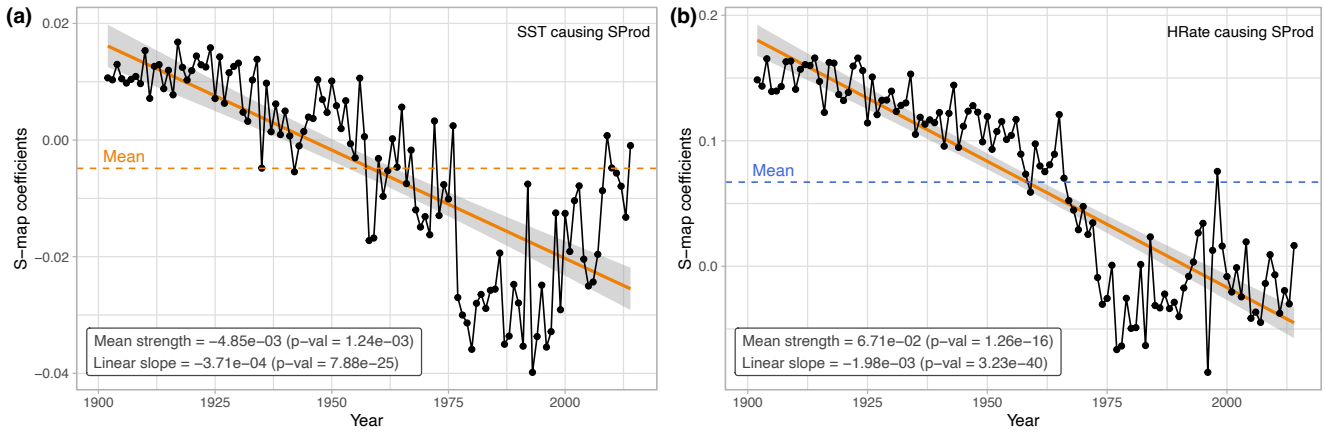

Figure 3: S-map coefficients along time for the causality from SST to SProd and from Rate to SProd for the stock *hina rockfish Southern Pacific oast.* Both t-tests and linear regressions are considered significant, providing a negative mean of 4.85×1 ^{3} and a decreasing trend of 3.71×1 ^{4} year for the causality from **SST** to **SProd**, and a positive mean of 6.71×1 ^{2} and a decreasing trend of 1.98×1 ^{3} year for the causality from **SST** to **SProd**. The values are without the unit of the variables since they are scaled for the S-map forecasting. This could be interpreted as a negative effect of **SST** on **SProd** on average being more negative along time, and a positive effect of **Rate** on **SProd** being smaller along time.

RESULTS

Causality assessments in fish stock trajectories

The Convergent Cross-Mapping (CCM) analysis was applied to a dataset of 155 fish stocks to identify causal relationships between stock productivity and its potential drivers: fishing pressure (**Rate** harvest rate) and sea surface temperature (**SST**). The results, summarized in Figure 4a, indicate that fishing pressure (harvest rate) was the most frequently detected causal driver of productivity (**SProd**). A significant causal link from harvest rate to productivity (**Rate** to **SProd**) was identified in 73 of the 155 stocks analyzed. In contrast, a causal influence of **SST** on productivity (**SST** to **SProd**) was found in 41 stocks. The analysis also tested for reverse causality, finding that productivity was a driver of harvest rate in 65 stocks and of **SST** in only 19 stocks, suggesting that drivers primarily influence productivity rather than the other way around. Figure 4b shows the distribution of causality detection results across 155 fish stocks, categorized by the drivers that showed significant causal relationships with stock productivity. Among stocks with detectable causality, harvest rate emerged as a more prevalent driver than SST: 42 of stocks showed causality only with harvest rate,

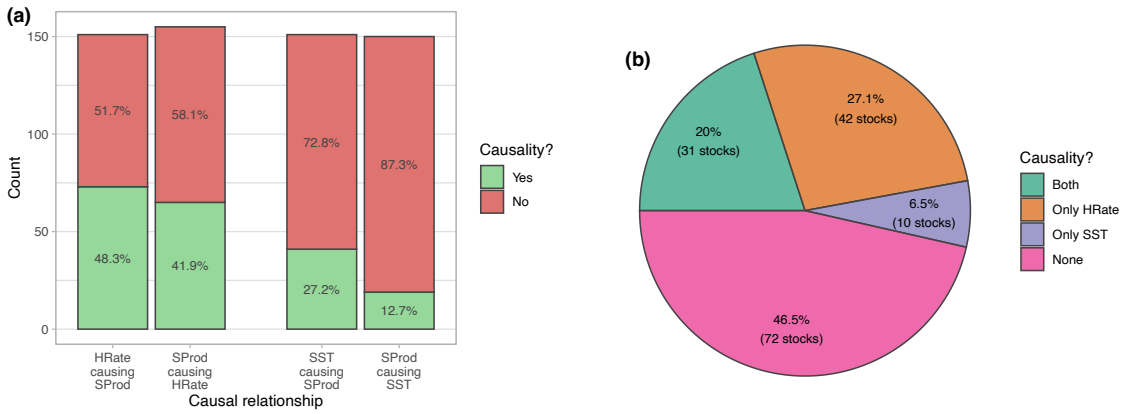

Figure 4: Convergent Cross-Mapping results for the detection of causal relationships. (a) Stacked bar plot of the number of stocks where the causality is assessed for each causal relationship tested. Causality was deemed irrelevant for 4 stocks for **SST** causing **SProd** and **Rate** causing **SProd**, and for 5 stocks for **SProd** causing **SST**. In these cases, the library variable (consequence variable, here **SProd** and **SST**) did not provide a reliable embedding, as indicated by negative forecasting skill in the Simplex projection. (b)

while 10 exhibited causality only with SST. A smaller proportion of stocks (31) demonstrated significant causal relationships with both environmental drivers.

Estimations of causal signs and trends

Following the detection of causal links of Sea Surface Temperature (**SST**) and harvest rate (**Rate**) on stock productivity (**SProd**), a multivariate S-map analysis was conducted to quantify the strength, sign, and temporal trend of these relationships Figure 5. Of the stocks analyzed, a majority (22 stocks) showed a significantly negative average effect of **SST** on **SProd** (Figure 5). In contrast, 11 stocks exhibited a positive effect, and 8 showed no significant average sign. The strength of the causal link from **SST** to **SProd** did not change significantly over time for 19 stocks. However, a notable number of stocks displayed a significant trend; the effect became increasingly negative over time for 14 stocks and more positive for 8 stocks. The most common patterns, observed in 10 stocks each, was a significantly negative causal effect that remained stable over time, and a negative effect that grew significantly stronger (more negative) over the time series.

For the causal link from harvest rate to productivity, the S-map analysis indicated a mostly positive response among the stocks (Figure 5). A significantly positive effect of harvest rate on productivity was identified in 60 stocks, suggesting that for these populations, increasing fishing pressure was associated with higher productivity. Conversely, 9 stocks showed a significantly negative relationship, where higher harvest rates corresponded to lower stock productivity. For the remaining 4 stocks, the S-map coefficient for the effect of harvest rate was not statistically significant. The scatterplots of S-map coefficient mean strength and temporal slope (Figure 5cd) reveal that harvest rate effects on productivity for most are tightly clustered around zero with relatively modest temporal variation, whereas SST effects exhibit a tighter coefficient range. Together, these patterns indicate that both the mean effect and its temporal change are stronger for harvest rate than for SST in shaping stock productivity.

Spatially, the maps in Figure S1 revealed pronounced spatial heterogeneity in both the sign and temporal trend of the effects: for SST->SProd, many regional are dominated by negative coefficients that are either stable or becoming more negative, with positive or neutral slices occurring more sporadically across the global distribution. In regions with multiple assessed stocks such as the US West Coast, the Atlantic Ocean, and Australia, the SST signal tends to cluster in negative-stable or negative-decreasing categories, whereas regions represented by one or two stocks show mixed signs and trends that warrant cautious interpretation. By contrast, the HRate->SProd maps exhibit predominantly positive effects in many regionsoften with stable or increasingly positive trendswhile negative responses are present in a minority of areas and typically display stable or decreasing trends. Collectively, these spatial patterns underscore region-dependent dynamics in both sign and trend, with clearer regional signals emerging where local sample sizes are larger and more heterogeneous mosaics where representation is sparse.

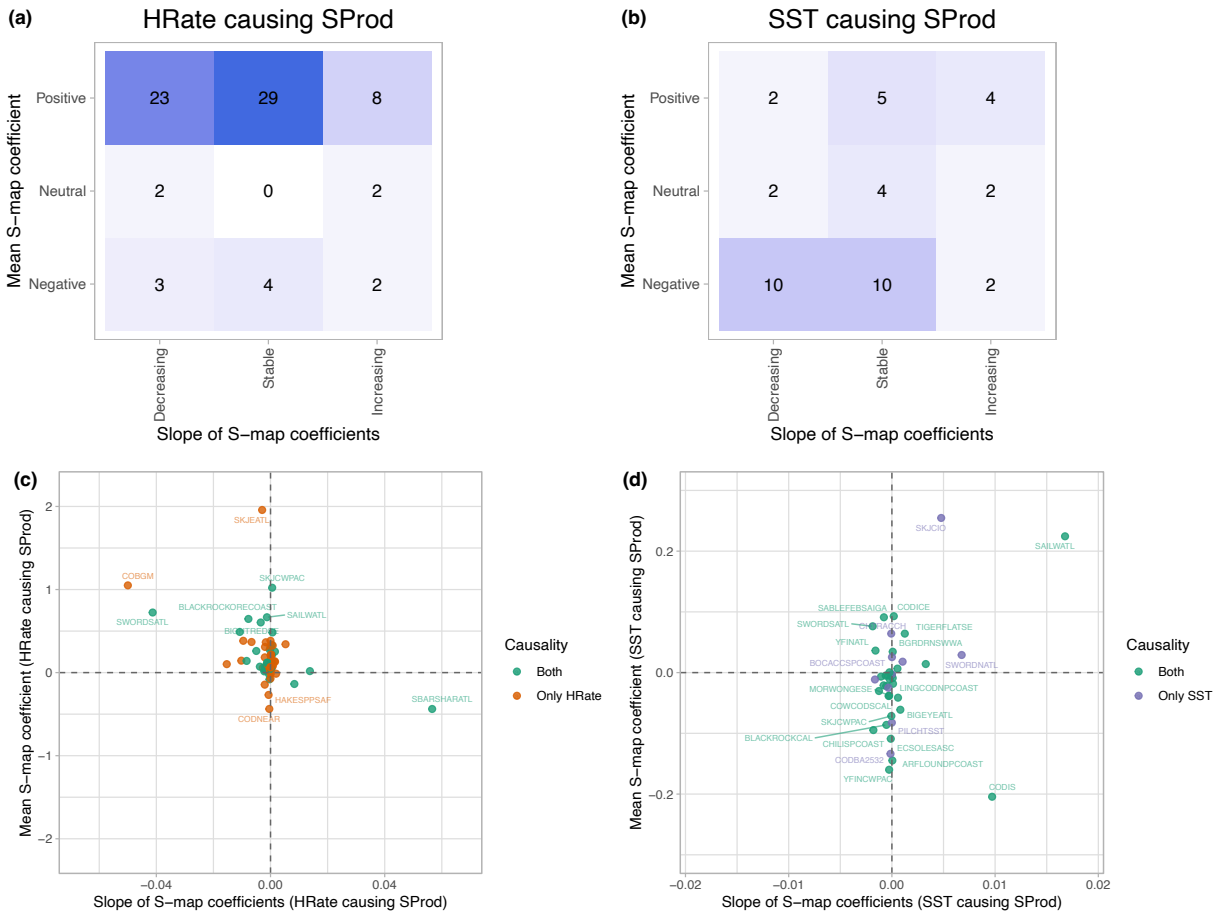

Figure 5: Sign and trend of the causal effects, resulting from the analysis on the multivariate S-map. These results are only provided for stocks where causality was assessed (Figure 4). (a,b) Sign and trend of the S-map coefficients, for the causal relationship from Rate to SProd (a) and from SST to SProd (b). (c,d) Scatter plots of the sign vs trend of the S-map coefficients for each stock, for Rate causing SProd (c) and SST causing SProd (d). Labels in the graph are stock IDs.

DISCUSSION

This study applied a data-driven framework to assess the causal effect of fishing pressure and warming on fish stock productivity on a global scale. Using Empirical Dynamic Modeling (EDM), our analysis showed that the causal effect of both drivers varies by stock, but identified harvest rate as the most prevalent driver of stock productivity, a finding that aligns with expert assessments identifying direct exploitation as the primary factor impacting marine ecosystems[4,26]. The influence of Sea Surface Temperature (SST) was detected in a substantial number of stocks (x%), providing data-driven evidence that climate forcing directly impacts the productivity of fisheries. These results underscore the value of equation-free methods for disentangling the complex, non-linear interactions that govern fisheries dynamics, moving beyond traditional models that may struggle to capture such complexity[16,27,28].

Our analysis of the quantified causal effects revealed distinct patterns for management. The influence of harvest rate on productivity was divided: for some stocks, higher fishing pressure was linked to increased productivity, while for others, it was associated with a decline. This dual effect is consistent with fisheries theory, where productivity may initially rise with exploitation before declining as a stock becomes overfished[29,30]. However, a mean positive Smap coefficient doesn't necessarily mean that keeping fishing pressure will continue having a positive effect. As shown for the China Rockfish Southern Pacific Coast stock in Figure 3, where the sign of the Smap coefficient is significantly positive on average, but it crashes in the 70s, reaching negative values. This highlights the relevance of assessing both the overall causal strength and its trend over time. More critically, the effect of SST on productivity was predominantly negative and, for many stocks, was found to be intensifying over time. This trend suggests that the adverse impacts of ocean warming on fish stocks are not only present but are becoming stronger, posing a growing threat to fisheries sustainability

and food security[7,31,32]. This dynamic, non-stationary nature of environmental impacts highlights the limitations of static management approaches and points to the need for adaptive strategies that can account for changing environmental baselines[33].

Our findings on SST causality reveal several patterns when examined alongside previous research. Pierre et al. (2018)[17] analyzed the causal link between SST and Recruitment (R) for 17 stocks, identifying significant relationships in 10 cases. When applying our more stringent approach to the same SST -> R causal link, we detected causality only for Eastern Atlantic bluefin tuna (*Thunnus thynnus*). This result reflects the conservative nature of our methodology. Our primary analysis examined the link between SST and productivity (SProd) across multiple fish stocks. We detected causal relationships for Baltic cod (*Gadus morhua*) and Irish Sea cod, consistent with findings by Pierre et al. for these species. For Iceland cod, we identified an SST -> SProd link that had not been previously reported. However, several stocks showed no detectable SST -> SProd relationship in our analysis, including Barents Sea cod, North Sea plaice (*Pleuronectes platessa*), and Arctic pollack (*Pollachius virens*). For Eastern Atlantic bluefin tuna, direct evaluation of SST -> SProd links was not possible due to data limitations in our final dataset (Supplementary Table S1). The methodological approach employed in this study differs from previous work in its validation framework. Both studies utilize Convergent Cross-Mapping (CCM), but our method incorporates an additional validation step: comparing observed forecast skill against null models generated from time-shuffled surrogates. This dual-test approach provides more stringent causality assessment, which accounts for the reduced number of significant causal links detected compared to methods that rely solely on convergence trend analysis.

While our approach offers a robust, equation-free method for assessing fishery dynamics, it is not without limitations. EDM methods are sensitive to time series length and the magnitude of observation error; they perform best with long time series and may struggle to resolve complex dynamics in short datasets or for species with lifespans longer than the available data[19,34]. Our analysis was also restricted to testing harvest rate and SST as drivers, while other factors such as predator-prey interactions, habitat quality, or other environmental variables could also play crucial roles[4,11,25,28,35,36].

Despite limitations, this work provides a significant step toward integrating non-linear, data-driven insights into fisheries management. By quantifying the strength and trend of driver impacts, our results provide warnings of changing productivity regimes and help evaluate the efficacy of management actions. This is particularly valuable for species that are difficult to assess with traditional models, such as short-lived species with highly variable dynamics. Future research could benefit from testing a wider array of biotic and abiotic drivers tailored to specific ecosystems. By doing so, we can move closer to an ecosystem-based approach to fisheries management that is adaptive and resilient to the challenges of a changing climate[37–40].

DATA AVAILABILITY STATEMENT

Data and code are available in the Github repository at https://github.com/RaphBnrd/RAMLDB_causality/tree/main.

ACKNOWLEDGMENTS

This study was financially supported by JCJC ANR-22-CE32-0001-01.

AUTHOR CONTRIBUTIONS

Conceptualization: RB, VD & AVC, Methodology: RB, VD & AVC, Investigation: RB, Visualization: RB & AVC, Writing: RB, VD & AVC, Editing: RB, VD & AVC, Funding Acquisition: VD.

AUTHOR COMPETING INTERESTS

The authors have declared that no competing interests exist.

REFERENCES

[1] Food and Agriculture Organization of the United Nations. *The State of World Fisheries and Aquaculture 2024: Blue Transformation in Action*. FAO, Rome, 2024.
[2] Sarah Cooley, David Schoeman, Laurent Bopp, Philip Boyd, Simon Donner, W Kiessling, P Martinetto, E Ojea, MF Racault, B Rost, et al. *Oceans and coastal ecosystems and their services*. Cambridge University Press, 2023.
[3] Christopher M Free, James T Thorson, Malin L Pinsky, Kiva L Oken, John Wiedenmann, and Olaf P Jensen. Impacts of historical warming on marine fisheries production. *Science*, 363(6430):979–983, 2019.
[4] Mathieu Pélissié, Vincent Devictor, Olaf Jensen, and Vasilis Dakos. Ocean warming drives abrupt declines in fish productivity at global scale. *EcoEvoRxiv*, May 2025. Publisher: EcoEvoRxiv.
[5] Sévrine F Sailley, Ignacio A Catalan, Jurgen Batsleer, Sieme Bossier, Dimitrios Damalas, Cecilie Hansen, Martin Huret, Georg Engelhard, Katell Hamon, Susan Kay, et al. Multiple models of european marine fish stocks: Regional winners and losers in a future climate. *Global Change Biology*, 31(4):e70149, 2025.
[6] Martha Teshome. Charting the systemic and cascading impacts of climate change on marine food systems and human health. *BMJ global health*, 8(Suppl 3), 2024.
[7] Daniel G Boyce, Derek P Tittensor, Cristina Garilao, Stephanie Henson, Kristin Kaschner, Kathleen Kesner-Reyes, Alex Pigot, Rodolfo B Reyes Jr, Gabriel Reygondeau, Kathryn E Schleit, et al. A climate risk index for marine life. *Nature Climate Change*, 12(9):854–862, 2022.
[8] Céline Bellard, Clara Marino, and Franck Courchamp. Ranking threats to biodiversity and why it doesnt matter. *Nature Communications*, 13(1):1–4, 2022.
[9] Eduardo Sonnewend Brondízio, Josef Settele, Sandra Diaz, and Hien Thu Ngo. *Global assessment report of the intergovernmental science-policy platform on biodiversity and ecosystem services*. IPBES, 2019.
[10] Gary P Griffith. Closing the gap between causality, prediction, emergence, and applied marine management. *ICES Journal of Marine Science*, 77(4):1456–1462, 2020.

[11] Stanislas Rigal, Vasilis Dakos, Hany Alonso, Ainars Auniņš, Zoltán Benkő, Lluís Brotons, Tomasz Chodkiewicz, Przemysław Chylarecki, Elisabetta De Carli, Juan Carlos Del Moral, et al. Farmland practices are driving bird population decline across europe. *Proceedings of the National Academy of Sciences*, 120(21):e2216573120, 2023.
[12] Daniel Ricard, Cóilín Minto, Olaf P Jensen, and Julia K Baum. Examining the knowledge base and status of commercially exploited marine species with the ram legacy stock assessment database. *Fish and fisheries*, 13(4):380–398, 2012.
[13] Ray Hilborn. Calculation of biomass trend, exploitation rate, and surplus production from survey and catch data. *Canadian Journal of Fisheries and Aquatic Sciences*, 58(3):579–584, 2001.
[14] Katyana A Vert-Pre, Ricardo O Amoroso, Olaf P Jensen, and Ray Hilborn. Frequency and intensity of productivity regime shifts in marine fish stocks. *Proceedings of the National Academy of Sciences*, 110(5):1779–1784, 2013.
[15] NAA Rayner, De E Parker, EB Horton, Chris K Folland, Lisa V Alexander, DP Rowell, Elizabeth C Kent, and A Kaplan. Global analyses of sea surface temperature, sea ice, and night marine air temperature since the late nineteenth century. *Journal of Geophysical Research: Atmospheres*, 108(D14), 2003.
[16] Sarah M. Glaser, Hao Ye, Mark Maunder, Alec MacCall, Michael Fogarty, and George Sugihara. Detecting and forecasting complex nonlinear dynamics in spatially structured catch-per-unit-effort time series for north pacific albacore (thunnus alalunga). *Canadian Journal of Fisheries and Aquatic Sciences*, 68(3):400412, March 2011.
[17] Maud Pierre, Tristan Rouyer, Sylvain Bonhommeau, and Jean-Marc Fromentin. Assessing causal links in fish stock–recruitment relationships. *ICES Journal of Marine Science*, 75(3):903–911, 2018.
[18] Floris Takens. Detecting strange attractors in turbulence. In *Dynamical Systems and Turbulence Warwick 1980: proceedings of a symposium held at the University of Warwick 1979/80*, pages 366–381. Springer, 2006.
[19] George Sugihara, Robert May, Hao Ye, Chih-hao Hsieh, Ethan Deyle, Michael Fogarty, and Stephan Munch. Detecting causality in complex ecosystems. *science*, 338(6106):496–500, 2012.
[20] ChunWei Chang, Masayuki Ushio, and Chihhao Hsieh. Empirical dynamic modeling for beginners. *Ecological Research*, 32(6):785796, May 2017.
[21] Henry B Mann. Nonparametric tests against trend. *Econometrica: Journal of the econometric society*, pages 245–259, 1945.
[22] Andreas Koutsodendris, Vasilis Dakos, William J. Fletcher, Maria Knipping, Ulrich Kotthoff, Alice M. Milner, Ulrich C. Müller, Stefanie Kaboth-Bahr, Oliver A. Kern, Laurin Kolb, Polina Vakhrameeva, Sabine Wulf, Kimon Christanis, Gerhard Schmiedl, and Jörg Pross. Atmospheric co2 forcing on mediterranean biomes during the past 500 kyrs. *Nature Communications*, 14(1), March 2023.
[23] George Sugihara. Nonlinear forecasting for the classification of natural time series. *Philosophical Transactions of the Royal Society of London. Series A: Physical and Engineering Sciences*, 348(1688):477495, September 1994.
[24] Ethan R. Deyle, Robert M. May, Stephan B. Munch, and George Sugihara. Tracking and forecasting ecosystem interactions in real time. *Proceedings of the Royal Society B: Biological Sciences*, 283(1822):20152258, January 2016.
[25] Masayuki Ushio, Chih-hao Hsieh, Reiji Masuda, Ethan R Deyle, Hao Ye, Chun-Wei Chang, George Sugihara, and Michio Kondoh. Fluctuating interaction network and time-varying stability of a natural fish community. *Nature*, 554(7692):360363, February 2018.
[26] Pedro Jaureguiberry, Nicolas Titeux, Martin Wiemers, Diana E Bowler, Luca Coscieme, Abigail S Golden, Carlos A Guerra, Ute Jacob, Yasuo Takahashi, Josef Settele, et al. The direct drivers of recent global anthropogenic biodiversity loss. *Science advances*, 8(45):eabm9982, 2022.
[27] Chih-hao Hsieh, Christian S Reiss, John R Hunter, John R Beddington, Robert M May, and George Sugihara. Fishing elevates variability in the abundance of exploited species. *Nature*, 443(7113):859–862, 2006.
[28] Hsiao-Hang Tao, Chih-hao Hsieh, Manuel Hidalgo, and Vasilis Dakos. Tracking changes in stability of north sea atlantic cod over 40 years. *ICES Journal of Marine Science*, 82(7):fsaf117, 2025.
[29] Nicholas J Barrowman and RA Myers. Is fish recruitment related to spawner abundance. *Fishery Bulletin*, 94:707–724, 1996.
[30] Ray Hilborn, Ricardo Oscar Amoroso, Christopher M. Anderson, Julia K. Baum, Trevor A. Branch, Christopher Costello, Carryn L. de Moor, Abdelmalek Faraj, Daniel Hively, Olaf P. Jensen, Hiroyuki Kurota, L. Richard Little, Pamela Mace, Tim McClanahan, Michael C. Melnychuk, Cóilín Minto, Giacomo Chato Osio, Ana M. Parma, Maite Pons, Susana Segurado, Cody S. Szuwalski, Jono R. Wilson, and Yimin Ye. Effective fisheries management instrumental in improving fish stock status. *Proceedings of the National Academy of Sciences*, 117(4):2218–2224, January 2020. Company: National Academy of Sciences Distributor: National Academy of Sciences Institution: National Academy of Sciences Label: National Academy of Sciences Publisher: Proceedings of the National Academy of Sciences.
[31] Daniel G Boyce, Derek P Tittensor, Susanna Fuller, Stephanie Henson, Kristin Kaschner, Gabriel Reygondeau, Kathryn E Schleit, Vincent Saba, Nancy Shackell, Ryan RE Stanley, et al. Operationalizing climate risk in a global warming hotspot. *npj Ocean Sustainability*, 3(1):33, 2024.
[32] Christopher M. Free, James T. Thorson, Malin L. Pinsky, Kiva L. Oken, John Wiedenmann, and Olaf P. Jensen. Impacts of historical warming on marine fisheries production. *Science*, 363(6430):979–983, March 2019. Publisher: American Association for the Advancement of Science.
[33] Christopher M Free, Tracey Mangin, Jorge García Molinos, Elena Ojea, Merrick Burden, Christopher Costello, and Steven D Gaines. Realistic fisheries management reforms could mitigate the impacts of climate change in most countries. *PloS one*, 15(3):e0224347, 2020.
[34] Charles T Perretti, Stephan B Munch, and George Sugihara. Model-free forecasting outperforms the correct mechanistic model for simulated and experimental data. *Proceedings of the National Academy of Sciences*, 110(13):5253–5257, 2013.
[35] Robert J Lennox, Marius Kambestad, Saron Berhe, Kim Birnie-Gauvin, Steven J Cooke, Lotte S Dahlmo, Sindre H Eldøy, Jan G Davidsen, Erlend M Hanssen, Lene K Sortland, et al. The role of habitat in predator–prey dynamics with applications to restoration. *Restoration Ecology*, 33(3):e14354, 2025.
[36] Mary E Hunsicker, Lorenzo Ciannelli, Kevin M Bailey, Jeffrey A Buckel, J Wilson White, Jason S Link, Timothy E Essington, Sarah Gaichas, Todd W Anderson, Richard D Brodeur, et al. Functional responses and scaling in predator–prey interactions of marine fishes: contemporary issues and emerging concepts. *Ecology Letters*, 14(12):1288–1299, 2011.
[37] Alejandro V Cano, Olaf P Jensen, and Vasilis Dakos. Identifying fish populations prone to abrupt shifts via dynamical footprint analysis. *Proceedings of the National Academy of Sciences*, 122(34):e2505461122, 2025.
[38] Marco Scotti, Silvia Opitz, Liam MacNeil, Axel Kreutle, Christian Pusch, and Rainer Froese. Ecosystem-based fisheries management increases catch and carbon sequestration through recovery of exploited stocks: The western baltic sea case study. *Frontiers in Marine Science*, 9:879998, 2022.
[39] KK Holsman, AC Haynie, AB Hollowed, JCP Reum, K Aydin, AJ Hermann, W Cheng, A Faig, JN Ianelli, KA Kearney, et al. Ecosystem-based fisheries management forestalls climate-driven collapse. *Nature communications*, 11(1):4579, 2020.
[40] Christian Möllmann, Xochitl Cormon, Steffen Funk, Saskia A. Otto, Jörn O. Schmidt, Heike Schwermer, Camilla Sguotti, Rudi Voss, and Martin Quaas. Tipping point realized in cod fishery. *Scientific Reports*, 11(1):14259, July 2021. Publisher: Nature Publishing Group.

SUPPLEMENTARY MATERIALS

Table S1: Comparison of causality assessment with Pierre et al. results

Species	Stock Pierre et al.)	Stock RAM)	SST to R Pierre et al.)	SST to R here)	SST to SProd here)
Clupea harengus	Irish Sea (VIIa)	HERRNIRS	FALSE	FALSE	FALSE
Clupea harengus	Norwegian spring spawning (NSS)	HERRNORSS	TRUE	NA	NA
Gadus morhua	Baltic (25-32)	CODBA2532	TRUE	FALSE	TRUE
Gadus morhua	Barents	CODNEAR	TRUE	FALSE	FALSE
Gadus morhua	Faroe	CODFAPL	FALSE	FALSE	FALSE
Gadus morhua	Iceland	CODICE	FALSE	FALSE	TRUE
Gadus morhua	Irish Sea (VIIa)	CODIS	TRUE	FALSE	TRUE
Gadus morhua	North Sea	CODIIIaW-IV-VIId	TRUE	NA	NA
Melanogrammus aeglefinus	Arctic	HADNEAR	FALSE	FALSE	FALSE
Melanogrammus aeglefinus	Faroe	HADFAPL	FALSE	FALSE	FALSE
Melanogrammus aeglefinus	North Sea	HADNS-IIIa	FALSE	NA	NA
Pleuronectes platessa	Irish Sea (VIIa)	PLAICIS	TRUE	FALSE	NA
Pleuronectes platessa	North Sea	PLAICNS	TRUE	FALSE	FALSE
Pollachius virens	Arctic	POLLNEAR	TRUE	FALSE	FALSE
Pollachius virens	Faroe	POLLFAPL	TRUE	FALSE	FALSE
Solea vulgaris	North Sea		FALSE	NA	NA
Thunnus thynnus	Eastern Atlantic	ATBTUNAEATL	TRUE	TRUE	NA

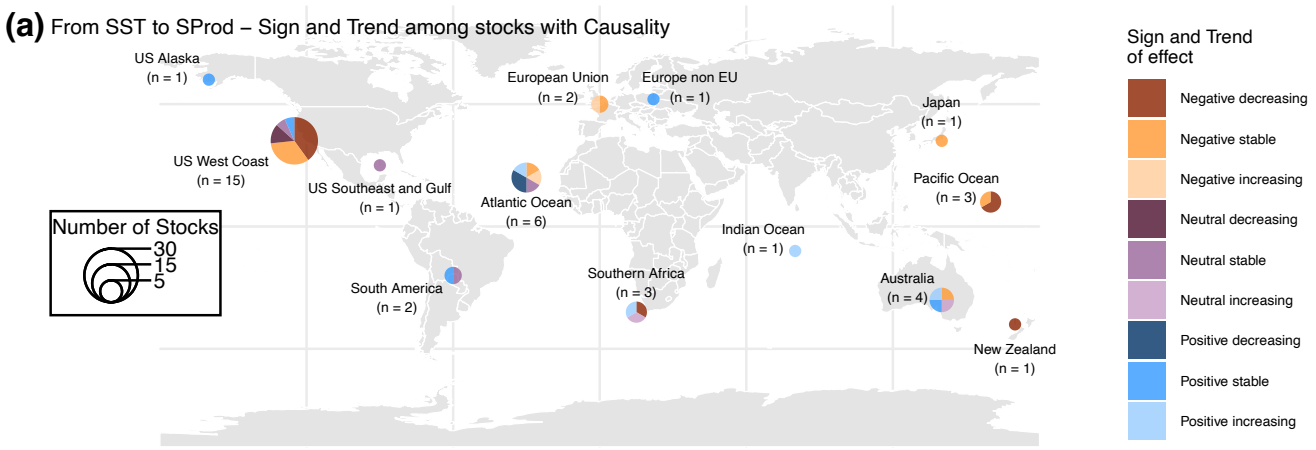

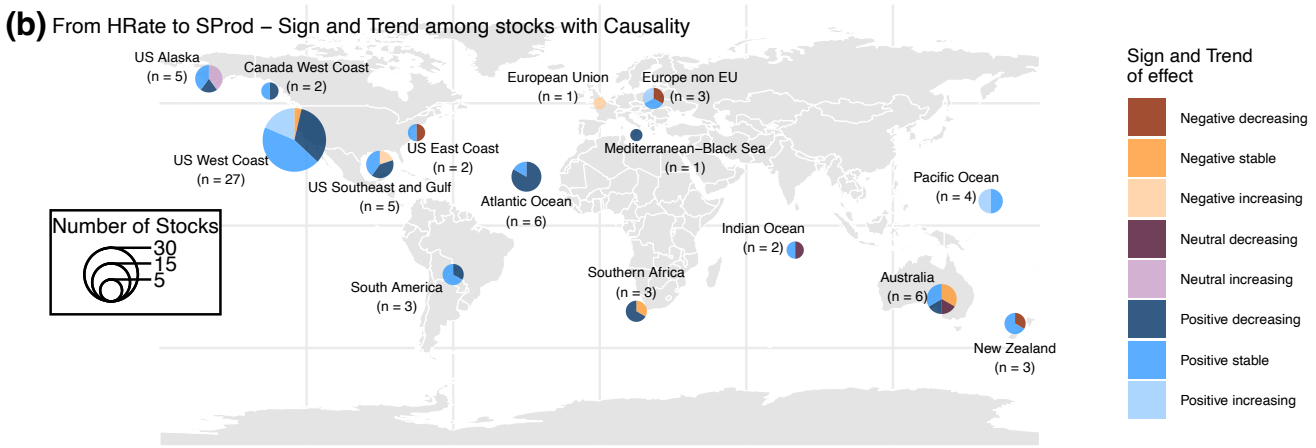

Figure S1: Spatial distribution of sign and trend of the causal effects, resulting from the analysis on the multivariate S-map. These results are only provided for stocks where causality was assessed (Figure 4). (b,c) Pie charts of the sign and trend of the causality located at the region of the fish stock, for the causal relationships from SST to SProd (b) and from Rate to SProd (c).